The ESO UVES Advanced Data Products Quasar Sample: Neutral Gas Mass and Metal Abundances in the Universe

Tayyaba Zafar[1]
Céline Péroux[2]
Giovanni Vladilo[3]
Miriam Centurión[3]
Paolo Molaro[3]
Valentina D'Odorico[3]
Kumail Abbas[4]
Attila Popping[5]
Bruno Milliard[2]
Jean-Michel Deharveng[2]
Stephan Frank[2,6]

[1] ESO
[2] Aix Marseille Université, CNRS, Laboratoire d'Astrophysique de Marseille (LAM), France
[3] INAF — Osservatorio Astronomico di Trieste, Italy
[4] Center of Excellence in Solid State Physics, University of the Punjab, Lahore, Pakistan
[5] International Centre for Radio Astronomy Research (ICRAR), The University of Western Australia, Crawley, Australia
[6] Department of Astronomy, Ohio State University, Columbus, USA

Damped Lyα absorbers (DLAs), seen in the spectra of background quasars, are unique probes to select HI-rich galaxies. We selected a dataset of 250 quasars observed with the Ultraviolet Visual Echelle Spectrograph (UVES) and available through the ESO UVES Advanced Data Products (EUADP) archive, to study the gas and metal properties of 150 damped absorbers. These high-redshift absorbers contain information on the physical state and chemical composition of the interstellar medium and the neutral gas mass, a possible indicator of gas consumption as star formation proceeds. We find no evolution of the neutral gas mass density, with sub-DLAs contributing 8–20 % (increasing with redshift). The EUADP dataset provides insights into the nucleosynthetic origin of nitrogen, confirming the bimodal behaviour of [N/α], and also confirms the deficiency of argon in DLAs.

Motivation

The study of quasar absorbers has contributed new insights into the field of galactic evolution research. The damped Lyα absorbers ($N_{HI} \geq 2 \times 10^{20}$ cm^{-2}) and sub-DLAs ($10^{19} \leq N_{HI} \leq 2 \times 10^{20}$ cm^{-2}; Péroux et al., 2005) contain a large fraction of neutral hydrogen in the Universe. DLAs are believed to be major contributors of the neutral gas in the Universe, so their study is an important tool for understanding the structure of young galactic systems. DLAs are frequently used as tracers of cosmic chemical evolution, despite the fact that their nature and morphology is still not clear. The metallicity distribution over cosmic time provides clues on the degree of chemical enrichment, the onset of initial star formation and the nature of galaxies.

We have collected UVES high-resolution quasar spectra taken between February 2000 and March 2007 and available in the EUADP archive, giving a sample of 250 quasar spectra (ranging from $0.2 < z < 6.3$). The total VLT–UVES exposure time of this dataset is 1560 hours. The individual quasar spectra have been carefully merged and normalised. To derive a complete census of DLAs/sub-DLAs both an automated and visual inspection have been undertaken, leading to a sample of 93 DLAs and 57 sub-DLAs. An extensive search in the literature indicated that 19 DLAs/sub-DLAs have had their HI column densities measured for the first time; four DLAs and six sub-DLAs are new identifications (see Zafar et al., 2013a).

The motivation behind the project is to obtain a complete picture of the redshift evolution of both the cosmological neutral gas mass density and the metal content of the Universe using both DLAs and sub-DLAs. Moreover, this dataset will help to perform studies of metal abundances, molecules, and advance understanding of the elemental nucleosynthetic origin. In addition, these studies will demonstrate the properties and environments of quasar absorbers. In this article, we summarise the early results from the EUADP dataset.

Neutral gas mass density

Baryons comprise a small fraction of the critical matter–energy density of the Universe with $\Omega_b h^2 = 0.02205 \pm 0.00028$. In recent years, new observations have considerably changed the global picture of the observable baryons in the Universe (e.g, Shull et al., 2012; Noterdaeme et al., 2012). In their neutral and molecular phases, baryons are the reservoirs of gas from which stars form. The HI clouds form molecules and molecular clouds further cool, fragment, and initiate star formation in galaxies. The neutral gas mass density (Ω_g) evolution over cosmological scales is a possible indicator of gas consumption as star formation proceeds. Ω_g observed in high-redshift quasar absorbers is expressed as a fraction of today's critical density. The contribution of sub-DLAs to Ω_g was however poorly constrained until now (see Péroux et al., 2005). Simulations indicate that the gas in sub-DLAs is located in extended halos, whereas the gas in DLAs is located in dense and compact regions (van de Voort et al., 2012). DLAs/sub-DLAs provide the reservoir of neutral gas and serve as a barometer of recent star formation activity.

We have built a carefully selected subset of the EUADP dataset to study the statistical properties of DLAs and sub-DLAs, their column density distribution and the contribution of sub-DLAs to the gas mass density. We combined our DLA and sub-DLA statistical samples with the Péroux et al. (2003) and Péroux et al. (2005) samples respectively, for improved statistics. The details on building the statistical sample are provided in Zafar et al. (2013b). On account of the high spectral resolution of EUADP, the hydrogen column density distribution, $f_{HI}(N,z)$, down to log $N_{HI} = 19.0$ is determined (Figure 1). The column density distribution, $f_{HI}(N,z)$, describes the evolution of quasar absorbers as a function of atomic column density and redshift.

The flattening of $f_{HI}(N,z)$ in the sub-DLA regime is present in the observations. We divided the $f_{HI}(N,z)$ distribution into two redshift bins of $1.5 < z < 3$ and $3 < z < 5$ (see Zafar et al., 2013b). A redshift evolution of $f_{HI}(N,z)$ is seen, indicating the presence of more sub-DLAs at high redshift compared to low redshift. Such an evolution suggests that sub-DLAs may merge and/or be more self-shielded with cosmic time. The behaviour of $f_{HI}(N,z)$ at six redshift bins (step increase of $z = 0.5$) is further used to determine the total HI gas mass density, Ω_g, between $1.5 < z < 5.0$. The results indicate
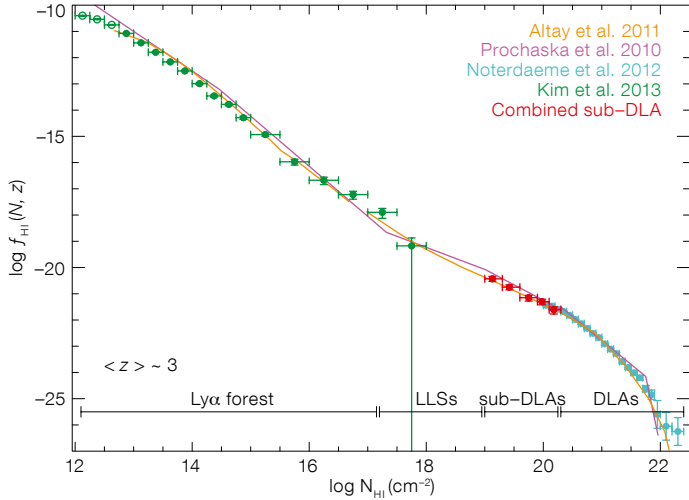
Figure 1. The column density distribution at $z \sim 3$ is plotted against $\log N_{HI}$ (from Zafar et al., 2013b). The red data points indicate $f_{HI}(N, z)$ for sub-DLAs. The green points represent $f_{HI}(N, z)$ for Lyα forest (Kim et al., 2013), the cyan points results from Noterdaeme et al. (2012) and the solid magenta line the estimation of $f_{HI}(N, z)$ at $z \sim 3.7$ using a series of six power laws by Prochaska et al. (2010). The solid orange line is the model prediction at $z \sim 3$ (Altay et al., 2011).
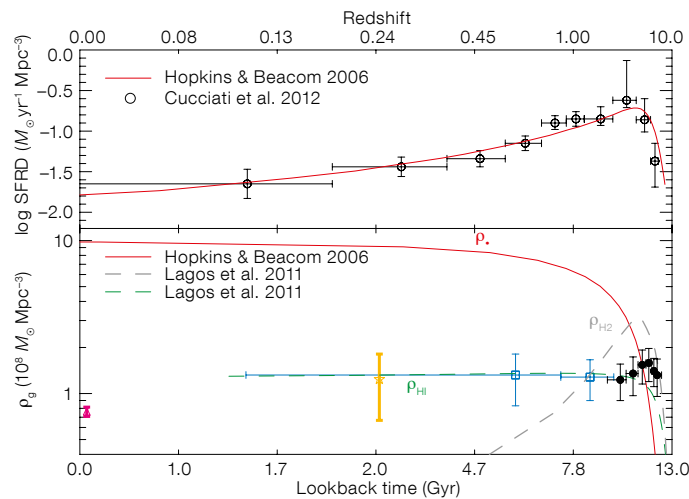

Figure 2. Upper panel: Total star formation rate (SFR) density as a function of lookback time (from Cucciati et al., 2012) is shown in black open circles. The red curve corresponds to the parametric form of the SFR density (Hopkins & Beacom, 2006). Lower panel: The black bins correspond to ρ_g measured from DLAs + sub-DLAs (Zafar et al., 2013b). See text for more details.

Evidence of bimodality in the nitrogen abundance distribution

The EUADP damped absorber dataset has been further used to understand the nucleosynthetic histories of nitrogen. N abundance determination in sites of low and high metallicities plays an important role in understanding its nucleosynthetic origin. The main pathway for the production of N in stars happens in the stellar H-burning layer, with the result that N is synthesised from C and O. Nitrogen has two production pathways, labelled either primary or secondary, depending on whether the seed C and O are produced by the star itself (primary) or were already present in the interstellar medium (ISM) out of which the star first condensed (secondary). Secondary production is the dominant process in the H-burning layers of intermediate-mass stars. Secondary production dominates at high metallicities ([O/H] > −1) and shows a correlation between (N/O) and (O/H). At low metallicities, N goes in lockstep with O, so that (N/O) remains approximately constant.

Primary N production in intermediate-mass stars occurs from the synthesis of C and O freshly produced by the star in the He-burning shell during the asymptotic giant branch (AGB) phase (Henry et al., 2000). In the case of massive stars, the N production is very uncertain. At very low metallicities, only fast-rotating massive stars ($9 \leq M/M_\odot \leq 20$) can provide primary N (Chiappini et al., 2006). The discovery of metal-poor halo stars with high (N/O) ratios seems to confirm the primary N production in massive stars (Spite et al., 2005).

Measurements of N abundance have been performed in different astrophysical sites. In partly ionised, HII regions of spiral and dwarf irregular galaxies (van Zee et al., 1998), metal-poor emission line galaxies (Nava et al., 2006), and HII regions in blue compact dwarf (BCD) galaxies (Izotov & Thuan, 2004), (N/O) ratios show a primary plateau at low O abundances and a secondary behaviour for [O/H] > −1.

Studies of nitrogen in DLAs/sub-DLAs (spanning the broad metallicity range $-3.0 \leq Z/Z_\odot \leq -0.5$) provide important

that sub-DLAs are important at all redshifts and their contribution to Ω_g increases from 8–20 %, with an increasing fraction at higher redshift.

In the lower panel of Figure 2, the trend of the physical space density, ρ_g, measured from DLAs/sub-DLAs, with lookback time is plotted. The magenta triangle represents the result for local galaxies from Martin et al. (2010). The orchid star illustrates ρ_g measured from the star-forming galaxies (Lah et al., 2007). The blue squares represent measurements from Mg II selected DLAs (Rao et al., 2006). The dashed green and grey lines represent the prediction of ρ_g and ρ_{H_2} (Lagos et al., 2011), respectively. The solid red line illustrates the evolution of stellar mass density build-up inferred from the star formation history by Hopkins & Beacom (2006).

Figure 2 shows no evolution of Ω_g (or ρ_g) from low- to high-redshift with $\Omega_g \sim 1 \times 10^{-3}$ or $\rho_g \sim 1.4 \times 10^8 M_\odot$ Mpc^{-3}. In contrast, star formation in galaxies steadily increases towards $z \sim 2.1$ by almost an order of magnitude (e.g., Cucciati et al., 2012). Given the star formation rate (SFR) density as function of redshift (Figure 2, upper panel), it is expected that HI plus H$_2$ gas at high redshift would be exhausted on timescales of few Gyr. However, the lack of evolution of Ω_g indicates that star formation alone cannot explain this nonevolution (Figure 2). Introduction of the continuous replenishment of gas through the accretion of matter from filaments and/or recombination of ionised gas in the walls of super-shells may help to sustain constant Ω_g over cosmic time (see Zafar et al., 2013b; Hopkins et al., 2008).

clues of the earlier stages of galactic chemical evolution. We have estimated nine new neutral N (NI) measurements and nine limits in DLAs/sub-DLAs from the EUADP sample (see Zafar et al., 2014a). We combine these data with a careful reappraisal of literature high-resolution measurements published to date, making a sample of 108 systems. This is the largest N abundance sample studied so far.

We also derived [N/α] (where α is an α-chain element, either O, S or Si) abundance ratios for our sample. The extended sample confirms the bimodal behaviour of [N/α] suggested in previous studies. Three quarters of the systems show ⟨[N/α]⟩ = −0.85 (± 0.20 dex) and one quarter are clustered at ⟨[N/α]⟩ = −1.41 (± 0.14 dex). In Figure 3, the magenta diamonds and green pluses indicate measurements in the HII regions of spiral (van Zee et al., 1998) and BCD galaxies (Izotov & Thuan, 2004) respectively (with average error bars indicated in the top-left corner). The high [N/α] plateau is consistent with the HII regions of BCD and dwarf irregular galaxies, although extended to lower metallicities, and could be interpreted as the result of a primary N production by intermediate-mass stars (see Figure 3). The low [N/α] values are the lowest ever observed in any astrophysical site. These low abundances may indicate a primary N production from fast-rotating, massive stars in relatively young or unevolved systems.

Deficiency of argon in DLA systems

The EUADP dataset has been further used to determine the ionisation state of the gas at different redshifts using the "noble gas" argon. This element, with first ionisation potential 15.76 eV, is expected to be mostly neutral in interstellar HI regions, which are opaque to photons with energies just above the HI ionisation threshold (13.6 eV). The ionisation fraction of Ar is very sensitive to high energy ionising photons that are able to leak through the neutral gas. When the radiation field is hard, Ar is predicted to be deficient relative to other low ionisation species typical of HI regions. On the other hand, Solar-like abundances are expected when the ionising spectrum is
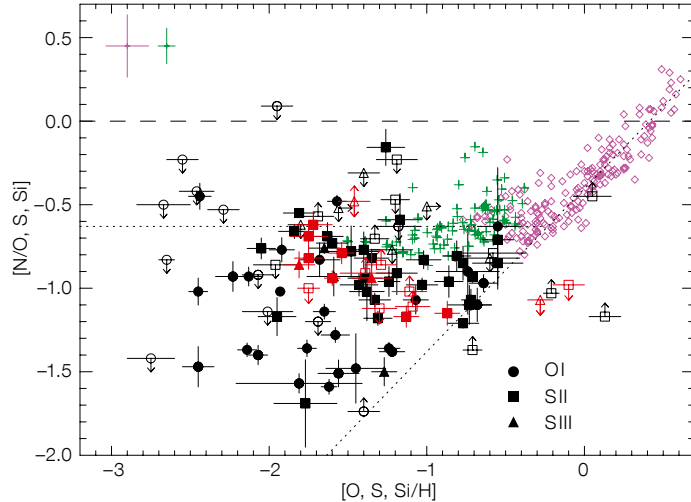

Figure 3. The [N/α] ratio determinations against metallicity. The circles, squares, and triangles indicate the O, S and Si abundances in DLAs/sub-DLAs, respectively (filled symbols: measurements; open symbols: limits). The red data points are the new estimates from Zafar et al. (2014a). Dotted lines are empirical representations of the secondary and primary N production. The dashed line indicates the Solar level.

soft. In the Galaxy, neutral argon is found to be deficient in low-density interstellar regions (Jenkins, 2013). However, owing to the saturation of neutral argon (ArI) lines, Galactic studies can only probe regions with relatively low HI column density, typically associated with warm interstellar gas. On account of the low metallicities of the DLAs, the rare ArI lines offer a way to probe the ionisation state of the neutral gas in high-redshift galaxies.

In Zafar et al. (2014b), we used the EUADP database to search for ArI lines in DLAs/sub-DLAs. We made three new measurements and obtained five upper limits of ArI. We combine these data with the literature high-resolution measurements, together comprising a total of 37 systems, i.e., the largest high-redshift Ar sample collected so far. We confirm that Ar is generally deficient in DLAs, with a mean value [Ar/α] ≈ −0.4 ± 0.06 dex (with α = S or Si). The [Ar/α] ratios show a weak, positive trend with increasing HI column density and increasing absorption redshift, and a weak, negative trend with metallicity, [S/H]. Detailed analysis of the measured abundance ratios indicates that the Ar deficiencies are due to ionisation processes, rather than dust depletion or nucleosynthesis. Altogether, the observational evidence is consistent with a scenario of Ar ionisation dominated by the harsh radiation of quasars, modulated by local HI self-shielding inside the DLA host galaxies.

In principle, by measuring the ionisation state of the gas at different redshifts, we

can track the evolution of the co-moving density of cosmic sources and variations of the transparency of the intergalactic medium resulting from the processes of cosmic reionisation. Our measurements and limits of Ar abundance suggest that the cosmic reionisation of HeII takes place at redshift higher than z ~ 3 (see Figure 4), but more measurements at z > 3.5 are required to set firmer constraints on the redshift evolution of the HeII reionisation.

Conclusions and prospects

Quasar absorbers are a useful tool to study the gas and metal enrichment history of the Universe. We have made use of the Advanced Data Products archive recently made available to the community by ESO to study the largest sample of quasar echelle spectra available to date. The EUADP sample of DLAs and sub-DLAs allows estimation of the neutral gas mass over cosmological scales. No evolution of the neutral gas mass density is indicated, which we interpret as the accretion of gas on cosmological scales. The EUADP dataset confirms the bimodal behaviour of [N/α], inferring primary N production by intermediate-mass stars. The EUADP study further confirms the deficiency of Ar in damped absorbers, interpreted as an ionisation effect, which indicates that the cosmic reionisation of HeII is completed above z ~ 3.

Further works, including the metallicity of sub-DLAs as possible tracers of the

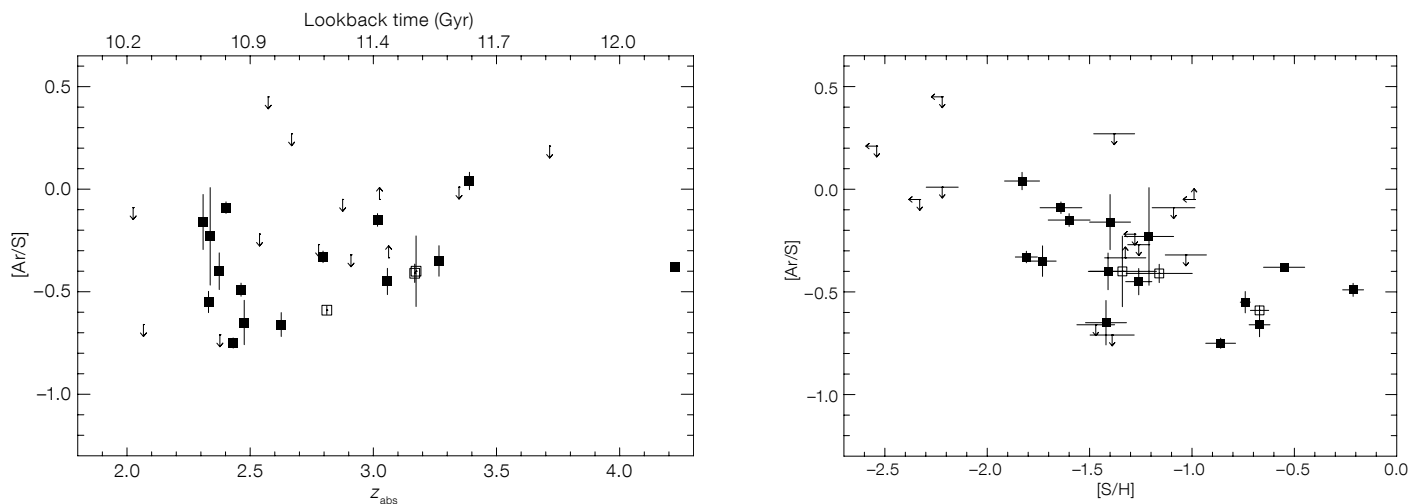Figure 4. Left panel: The [Ar/S] ratio in DLAs plotted against redshift (bottom axis) and lookback time (top axis), for $H_0 = 70$ km s^{-1} Mpc^{-1}, $\Omega_m = 0.3$, and $\Omega_\Lambda = 0.7$. Right panel: The [Ar/S] versus S-based metallicities in DLA systems. A small amount of chemical evolution can be seen in [Ar/S]. In both panels, solid squares and arrows correspond to measurements and limits, respectively. The open squares illustrate proximate DLAs with $z_{em} \approx z_{abs}$ (see Zafar et al. [2011] for more details).

circum-galactic medium of galaxies (Quiret et al., in prep), are underway. Finally, since we started this study, the number of quasar spectra available in the UVES Advanced Data Products archives has more than doubled. Altogether, these results illustrate the high scientific return of processed data archives.

References

Altay, G. et al. 2011, ApJ, 737, L37
Chiappini, C. et al. 2006, A&A, 449, L27
Cucciati, O. et al. 2012, A&A, 539, A31
Henry, R. B. C., Edmunds, M. G. & Köppen, J. 2000, ApJ, 541, 660
Hopkins, A. M. & Beacom, J. F. 2006, ApJ, 651, 142
Hopkins, A. M., McClure-Griffiths, N. M. & Gaensler, B. M. 2008, ApJ, 682, L13
Izotov, Y. I. & Thuan, T. X. 2004, ApJ, 602, 200
Jenkins, E. B. 2013, ApJ, 764, 25
Kim, T.-S. et al. 2013, A&A, 552, A77
Lagos, C. D. P. et al. 2011, MNRAS, 418, 1649
Lah, P. et al. 2007, MNRAS, 376, 1357
Martin, A. M. et al. 2010, ApJ, 723, 1359
Nava, A. et al. 2006, ApJ, 645, 1076
Péroux, C. et al. 2003, MNRAS, 345, 480
Péroux, C. et al. 2005, MNRAS, 363, 479
Prochaska, J. X., O'Meara, J. M. & Worseck, G. 2010, ApJ, 718, 392
Rao, S. M., Turnshek, D. A. & Nestor, D. B. 2006, ApJ, 636, 610
Spite, M. et al. 2005, A&A, 430, 655
van de Voort, F. et al. 2012, MNRAS, 421, 2809
van Zee, L. et al. 1998, AJ, 116, 2805
Zafar, T. et al. 2011, A&A, 532, A51
Zafar, T., Popping, A. & Péroux, C. 2013a, A&A, 556, A140
Zafar, T. et al. 2013b, A&A, 556, A141
Zafar, T. et al. 2014a, MNRAS, 444, 744
Zafar, T. et al. 2014b, MNRAS, 445, 2093Z

ESO/C. Snodgrass

B, V, R composite image of the barred spiral (SB) galaxy NGC 6300 taken with EFOSC2 on the New Technology Telescope (NTT). The active galactic nucleus of NGC 6300 is of Seyfert 2 type and displays rapidly variable hard X-ray emission. See Picture of the Week for 2 March 2015 for more information.

(Next page) Recent aerial view of the progress on levelling of the summit of Cerro Armazones in preparation for construction of the dome of the European Extremely Large Telescope.